MAGNETOHYDRODYNAMICS Vol. 51 (2015), No. 3, pp. 617–627

EXPERIMENTAL AND NUMERICAL INVESTIGATION OF THE ACOUSTIC ABSORPTION COEFFICIENT AT VERY LOW FREQUENCY

D.W.Y. Khoo, Y.A. Abakr

Department of Mechanical, Manufacturing and Materials Engineering,
The University of Nottingham Malaysia Campus,
Jalan Broga, 43500 Semenyih, Selangor Darul Ehsan, Malaysia
e-Mails: kedx1dkg@nottingham.edu.my, yousif.abakr@nottingham.edu.my

Sound attenuation had always been an interesting topic of investigation for many reasons. The range of frequency investigated by many researchers is usually of the order of tens of kHz, the lower frequency range investigated by some researchers, typically a few hundreds to few thousands of Hz, still falls far away from the interesting zone for the low frequency thermoacoustic engine, which is operating in a frequency range of 30–150 Hz, hence, this is considered a very low frequency range. Passive attenuation of acoustic waves was one of the important issues when creation of a travelling wave is intended. In order to experimentally simulate a thermoacoustic engine designed to utilise waste heat from cooking stoves as a source of electrical energy, a setup has been developed to represent the driver section of the engine. As a first step of the investigation, an acrylic straight tube configuration with a square cross-section is used to investigate the effectiveness of different absorbing materials by using multi-microphone impedance tube technique. Different passive attenuation options were tested. A hard end constructed of an 8 mm aluminium plate was used for validation. Different noise signals were tested, the uniform white noise was chosen over Swept sine signal because of its steady behaviour in the low frequency region. A Matlab program was created to calculate the absorption coefficient of the tested materials. The current study also includes the comparison with the results produced by the numerical simulation using DeltaEC. Results show the elastic aluminium termination end has better attenuation characteristics compared with the other alternatives. The outcomes of this work will be used for further ongoing investigations on loss assessments of the low frequency thermoacoustic engine. Moreover, the validated DeltaEC model will be used to investigate a wider range of alternative for better optimisation. The absorption coefficient can be improved by using a more elastic end and the optimum elasticity requirement will be optimised using DeltaEC simulation. A compliance volume integrated with an elastic end is also expected to work as a better alternative at very low frequency.

Introduction. The thermoacoustic engine is a device that converts heat to sound energy. Thermoacoustic engines work according to the Rayleighs criterion [1]. The SCORE$^{\text{TM}}$ thermoacoustic engine is a waste-heat driven travelling-wave engine that utilises the waste heat from a cooking stove to create travelling acoustic oscillations through a closed loop at an operating frequency of 30–150 Hz [2]. When a speaker is used to generate the sound waves at one of the termination ends in a straight tube, passive attenuation can be used to experimentally obtain a travelling wave in an open loop, simulating the conditions of the engine, while being able to control the frequency and amplitude of the wave. The travelling wave can be created by dissipating the sound energy using absorbing materials at another extremity of the tube. The sound absorption coefficient and the surface impedance are the two important indicators which can effectively determine how much sound energy is dissipated and reflected back. These acoustic properties can be determined if the sound reflection coefficient from a sample is known. There are several methods which can be used to determine the acoustic properties of a material with the aid of a commercial impedance tube setup. The well-known standing wave impedance tube method makes use of the measured standing wave ratio (SWR) for a specific frequency in the tube to determine the acoustic properties by means of only a movable microphone. The advantage of this method is that it is not necessary to calibrate the microphone. The disadvantages are the complex setup with a movable probe and the time needed to find the location of the maximum and minimum pressures [3].

An alternative way to measures the acoustic properties is by using two microphone systems, which require two similar microphones, fixed and phase-calibrated at different positions in the tube with a known distance between them [4–6]. Seybert and Ross [4] proposed a different method for impedance tube measurements of sound absorption using the pressure readings at two positions, called the two-microphone method, which was faster than the conventional standing-wave-ratio method. The acoustic wave response is mathematically separated into its reflection and incident components using a transfer function between the microphones. This decomposition of wave propagation allows the computation of the acoustic properties such as reflection coefficient, absorption coefficient and acoustic impedance. Chung and Blaser [5–7] further developed this method experimentally and later Chu [8, 9] also improved this method by including the tube-attenuation effect, allowing the microphones to be placed far away from the sample. Boden and Abom [10] studied the two-microphone method by using numerical simulations and found that this method had its lowest sensitivity when the two microphones were separated by a quarter wavelength. The influence of errors in the two-microphone method has been investigated [11–13]. Chu [14] has proven that in order to obtain accurate results, one of the microphones has to be placed close to a minimum pressure location, while the locations for the rest of the microphones are not as critical as long as the separation is not close to a half wavelength. The primary advantages of the two-microphone method are the significant time saving, no moving parts required, and its excellent suitability to quick response with a random noise source. The drawbacks are that its accuracy significantly degrades at large wavelengths (low frequencies) and at microphone separations near one-half wavelength (high frequencies). The two-microphone method has the added problems of requiring highly accurate microphone calibration [15].

There is a more recent acoustic properties measurement method utilising more than two microphones to carry out the measurements. This multi-microphone method, on the other hand, yields better results in the low frequency region. Fujimori *et al.* , Pope, Chu [16], Jones and Parrot [17] described the multiple-microphone method, a least square method on the pressure measurements at more than three positions. The multi-microphone method has also no restriction on microphones separation relative to wavelength and allows results to be plotted with a single line based on the transfer function of a few microphone combinations. Jang and Ih [18] theoretically and experimentally studied the influence of the microphone positions on the accuracy of the multiple-microphone method. They found that using equidistant positioning of microphones reduced errors within the effective frequency range. Moreover, they showed that the measurement accuracy could be increased and the frequency range could be widened by increasing the number of equidistant microphones. Another recent improved method uses least squares curve fitting to optimize the response of all the microphone positions to produce results with s minimum error [19, 20]. This paper will focus on measuring the acoustic properties using the least squares technique with the aid of a multi-microphone impedance tube system. The current study also includes the comparison with the results produced by the numerical simulation using DeltaEC [21].

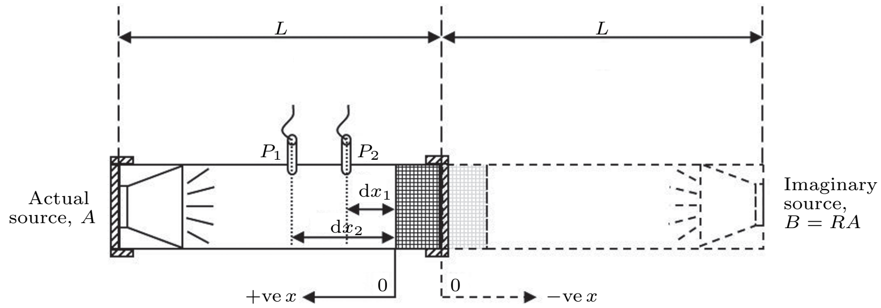

Fig. 1. The impedance tube setup for two-microphone method.

1. Least squares technique. The formulation of this method was developed based of an imaginary source equidistant from the specimen in an impedance tube but in the negative x-direction as depicted in Fig. 1.

The imaginary region is symmetrically mirrored at the end of the specimen from the actual source region. The amplitude of the imaginary source is given by

$$B = RA, \tag{1}$$

where R is the complex reflection factor and A represents the amplitude of the actual source in Eq. (1). The relationship between the measured pressure from each microphone and both of the sources can be deduced with the aid of a Greens function as shown in Eq. (2):

$$P_1 = Ag_{1A} + Bg_{1B} = A(g_{1A} + Rg_{1B}), \quad P_2 = Ag_{2A} + Bg_{2B} = A(g_{2A} + Rg_{2B}), \tag{2}$$

where P_1 and P_2 are the pressure readings from microphones 1 and 2, respectively. g_{1A} is the Greens function that relates the output of microphone 1 to the input of the actual source, A and g_{1B} is the Green function that relates the output of microphone 2 to the input of the imaginary source B. The same relationship applies for the Green functions g_{2A} and g_{2B} with respect to microphone 2. Considering a plane wave is propagating in the tube, the Green functions can be expressed by Eq. (3):

$$\begin{aligned} g_{1A} &= \frac{\rho_0 c}{2s} \mathrm{e}^{-jk(L-\mathrm{d}x_1)}, \quad g_{1B} = \frac{\rho_0 c}{2s} \mathrm{e}^{-jk(L+\mathrm{d}x_1)}, \\ g_{2A} &= \frac{\rho_0 c}{2s} \mathrm{e}^{-jk(L-\mathrm{d}x_2)}, \quad g_{2B} = \frac{\rho_0 c}{2s} \mathrm{e}^{-jk(L+\mathrm{d}x_2)}, \end{aligned} \tag{3}$$

where ρ_0 is the air density, c is the speed of sound, s is the cross-sectional area of the tube, L is the total length of the system, $\mathrm{d}x_1$ and $\mathrm{d}x_2$ are the distances between the sample and microphones 1 and 2, respectively. k represents the wave number which is defined as $2\pi f/c$. The transfer function H_{12} is the pressure ratio between microphones 1 and 2, which can be rearranged to give the complex reflection coefficient R, as shown in Eqs. (4) and (5):

$$H_{12} = \frac{P_2}{P_1} = \frac{g_{2A} + g_{2B}R}{g_{1A} + g_{1B}R}, \tag{4}$$

$$R = \frac{g_{2A} - g_{1A}H_{12}}{g_{1B}H_{12} - g_{2B}}. \tag{5}$$

The absorption coefficient and the surface impedance are the two important indicators which can effectively determine the fraction of energy that is dissipated and reflected back. The absorption coefficient of unity means the reflection coefficient is zero and all the incident energy is reflected back from the surface. The theory was initially applied to a two-microphone case. More microphones are needed to get a more accurate result. An optimized reflection coefficient R_{opt} can be obtained by using a least squares solution with the aid of the multi-microphone method. This optimized method will produce a single curve based on all the microphone combinations by taking the closest to the sample microphone as a reference.

$$R_{\mathrm{opt}} = -\frac{\sum_{m=2}^{M} (g_{1A}H_{1m} - g_{mA})(g_{1B}H_{1m} - g_{mB})^*}{\sum_{m=2}^{M} \left|g_{1B}H_{1m} - g_{mB}\right|^2}. \tag{6}$$

The purpose of this optimization is to minimize the sum of errors between the measured and the analytically derived pressure. Eq. (6) can be used for any number of microphones M, where m indicates the number of each microphone in the tube. The absorption coefficient α and the surface impedance Z_{s} of the sample can be determined by Eqs. (7) and (8), respectively:

$$\alpha = 1 - \left|R_{\mathrm{opt}}\right|^2, \tag{7}$$

$$Z_{\mathrm{s}} = Z_0 \left(\frac{1 + R_{\mathrm{opt}}}{1 - R_{\mathrm{opt}}}\right), \tag{8}$$

where $Z_0 = \rho_0 c$ is the acoustical characteristic impedance of the air. The surface impedance is a measure of the amount by which the motion induced by a pressure applied to a surface is impeded. Another acoustic property which can be used to present the characteristic of the materials is the complex specific acoustic impedance ratio. The specific acoustic impedance ratio is obtained by dividing Z_{s} by Z_0. The real part describes energy losses, whereas the imaginary part indicates phase changes caused by the materials.

2. Experimental setup. The experimental apparatus is composed of straight tubes and tapers made from transparent acrylic plates. The total length of the system is 2.85 m and the wall thickness is 5 mm. The straight tubes have an internal square cross-sectional area of $0.0081\,\mathrm{m}^2$ and the tapers have an internal rectangular cross-sectional area of $0.0122\,\mathrm{m}^2$, respectively. Tapers are used at two ends of the tube to reduce energy losses and smooth the acoustic flow. The working fluid is the air at atmospheric pressure. One extremity of the tube is attached to a loudspeaker which acts as an acoustic excitation source, while the tested sample is placed inside a wooden speaker box which is used as an absorbing termination at the other end. The loudspeaker generates an excitation signal which propagates down the tube and reflects from the other end of the tube with the aid of an amplifier, whereas the tested sample in the wooden speaker box allows a different termination impedance to be altered in order to match with the waveguide impedance to generate a travelling wave which propagates down the tube.

The voltage supply to the loudspeaker is maintained at 2 V producing an acoustic power of about 0.2–0.4 W for all tested frequencies. An elastic gasket is used between the tubes and the tapers as well as the speaker boxes to provide sealing and avoid air leakage. A total of six microphones are used to measure the sound pressure along the length of the tube with the aid of a data acquisition system. Holes are drilled on the top side of the straight tubes and tapers

(a) (b) (c) (d)

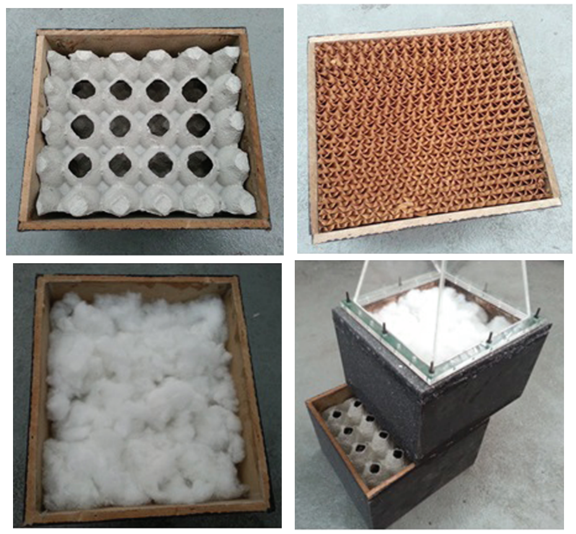

Fig. 2. Four different types of materials under investigation: (*a*) egg tray, (*b*) honeycomb, (*c*) sponge and (*d*) egg tray and sponge combination.

whereby the microphones can be slotted in and out easily to carry out the measurement. The microphones are sealed tightly to the mounting holes by using a rubber and O-ring. All the microphones have different sensitivity and it is important to calibrate these microphones with a sound calibrator for every experimental run. The Labview software was used to collect and store the data at a rate of 10 kHz. Moreover, the post-processing of data was done using the Matlab software. The acoustic properties are measured by varying the materials in the wooden speaker box. There are basically three different types of absorbing materials, as shown in Fig. 2: sponge, honeycomb filter and egg tray. The experiment was conducted with empty wooden speaker boxes, which are believed to give a compliance volume. An 8 mm aluminium plate was also used as a rigid backing for verification purpose.

At the beginning, the present study examined 3 different types of excitation signals, namely, Uniform white noise, Gaussian white noise, and Swept sine signal. The measurements were made using a source of uniform white noise and repeated with a Gaussian white noise having a wide frequency band. The uniform white noise produces a uniformly distributed random signal with a constant amplitude of unity, whereas the random signals produced by Gaussian white noise is not systematically planned and the amplitude tends to vary with time because it relies on the mean and variance of the normally distributed signals. A swept sine signal is characterised by the continuously increasing or decreasing frequency with time, while the amplitude is constant. To preoccupy the investigation in the low frequencies, the frequency band in the time domain for the Swept sine signal was adjusted so that a measurement can be taken accurately in the low frequency region.

3. Impedance tube method. An impedance tube provides an effective and easy way for measuring the acoustic properties of the tested specimen. This method has a frequency limitation as a consequence of the microphone positions. The working frequency range of interest is crucially important and dictated by the shortest and farthest microphone separations. If the microphones are too close together, the pressure difference between them will be too small to be accurately measured and the errors will increase. The impedance tube system needs to be long enough, with the farthest microphone separation of approximately 1/20th of the wavelength at the lowest required frequency of measurement. The low frequency limit is given by Eq. (9):

$$f_{\mathrm{l}} > \frac{0.05c}{|z_1 - z_2|}. \tag{9}$$

This method is also sensitive to errors if the microphones are too far apart. As the distance between the microphones becomes equal to the wavelength, the pressure at the two microphones will be the same at the corresponding frequency and the simultaneous equations will not be solvable. The upper frequency limit is given by Eq. (10):

$$f_{\mathrm{u}} < \frac{0.45c}{|z_1 - z_2|}. \tag{10}$$

In addition, the microphone closest to the loudspeaker should be at least two tube diameters from the loudspeaker as by this point any cross modes generated will be ceased to be in effect so that only plane waves will be incident on the sample. The closest to the sample microphone should also be sufficiently far from the sample. To ensure accurate measurements, at least a distance of half of the diameter of the tube is needed in between. The reason for using the multi-microphone method in this work is due to the fact that additional microphones increase the working frequency range and it is also possible to compute the transfer functions separately for each pair of microphone positions.

4. DeltaEC$^{\mathrm{TM}}$ modelling and simulation. Design Environment for Low-Amplitude ThermoAcoustic Energy Conversion (DeltaEC) is a computer program that calculates details of how thermoacoustic equipment performs, or can help the user to design equipment to achieve the desired performance. DeltaEC is used to calculate a variety of complicated thermoacoustic devices with a low pressure amplitude. It solves the wave equation in a gas or liquid, in a geometry given by the user as a sequence of segments, such as ducts, compliances, transducers, and thermoacoustic stacks or regenerators. A solution to the appropriate one-dimensional wave equation is found in each segment, with pressures and volume flow rates matched at the junctions between segments. The software uses a system of "guesses" and "targets", the former being generally uncontrolled parameters such as frequency or pressure amplitude, and the latter being parameters that can be controlled, such as lengths or boundary conditions. The suitable selection of 'guesses' and 'targets' is the key to the successful use of the program; the program will iteratively adjust the variables listed as 'guesses' to achieve the 'target' values. The model is constructed by eighty three segments including the six RPN segments used to indicate the microphone locations and sixty three RPN segments after the HARDEND for the calculations of least squares technique. The impedance tube system is made of six CONE segments and six DUCT segments. A total number of two GUESSes and two TARGETs is chosen. The first segment (zeroth segment) is always a BEGIN segment and will be used as a loudspeaker that generates a sinusoidal wave in this case. This segment contains global variables such as mean pressure, frequency, mean temperature and gas type. Calculations have been done using the mean pressure $P_m = 1$ bar, the mean temperature $T_m = 300\,\mathrm{K}$ and an acoustic pressure of 50 Pa. The air was used as a working gas. Perspex is selected as the material for the components in the model with the aid of User Defined Function (UDF). The HARDEND acts as a rigid backing to reflect the acoustic wave. The GUESS vector, which has two components in this case, shows which variables DeltaEC targets for a solution: the frequency and the volume flow rate.

The initial guess of the frequency is 20 Hz and the initial value of the volume flow rate is 0.005 m/s.

5. Results and discussion. In the range of the tested frequency, the type of the input signal was found to be of small effect on the reflection and absorption coefficients, which is a good evidence of the validity of the experimental setup. Fig. 3 presents the reflection and absorption coefficients of the rigid plate for different types of excitation signal from the source. The aluminium plate was found not to be a perfect rigid backing, but the reflection coefficient was close to unity in the tested frequency range. Furthermore, the swept sine signal showed deviation from all other signals and the numerical simulation in the low frequency range up to about 65 Hz, but the reflection coefficients for all types of signals behave in a similar manner elsewhere. The numerical results produced by DeltaEC were found to be in an excellent agreement with the experimental results throughout the entire frequency range. However, the coefficients were slightly overestimated by the numerical simulation at a frequency above 120 Hz, this is due to nonlinear effects not taken into consideration by the DeltaEC simulation.

After validation of the experimental setup against the DeltaEC simulation, in order to find a potential attenuation arrangement suitable for the very low frequency range (below 150 Hz), the performance of different material combinations was also under investigation. Therefore, eight different arrangements were investigated as well as the rigid aluminium plate which was taken as a reference. The absorption coefficient was found to change with the frequency for all types of

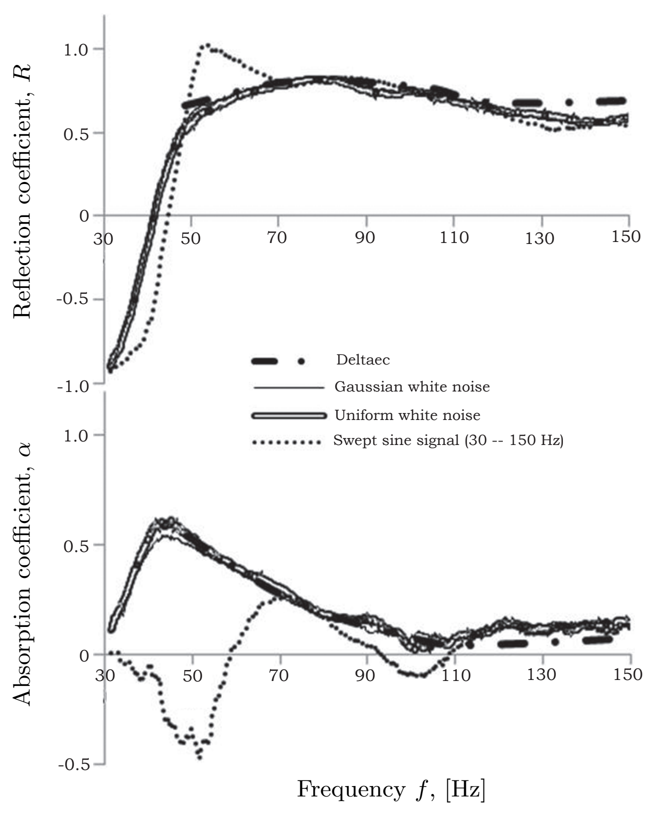

Fig. 3. Results for the reflection and absorption coefficients as a function of the frequency when an aluminium plate is used as the rigid backing.

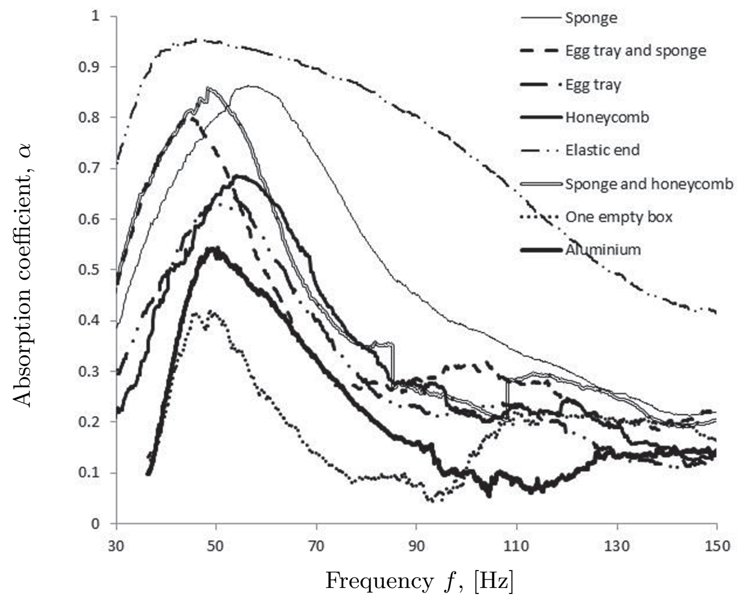

Fig. 4. The responses of the absorption coefficient as a function of the frequency for all tested materials when uniform white noise is used as the excitation signal.

attenuation arrangements. The elastic end showed the highest absorption coefficient relative to the other attenuation alternatives. The elastic end was an acrylic plate with a thickness of 8 mm. Other attenuation arrangements worked better at a higher frequency range, but for this very low frequency range, which is rarely investigated, the elastic end was found to be better, as shown in Fig. 4. A general trend can be observed that all the tested materials show a maximum absorption coefficient at a frequency of approximately 50 Hz. The absorption coefficient gradually decreased after the peak value with the increasing frequency. A compliance volume gives a rather low absorption coefficient if compared to the rigid end (aluminium plate) at the frequency below 100 Hz, whereas the absorption coefficient obtained for the rest of the absorbing material arrangements was higher than the rigid plate regardless of the frequency, which gives confidence in the validity of the results. Note that the aluminium plate is approximately a rigid end and should reflect most of the incident acoustic waves. Besides that, the sponge was found to have a lower absorption coefficient compared to the elastic end, but it has a better absorption coefficient compared to all other materials or combinations of materials used in the frequency range above 50 Hz. All combinations of two materials performed better in the frequency range below 50 Hz. With the inclusion of the sponge, all materials investigated exhibited a higher absorption coefficient when used in a combination of two materials together, compared with the case when each one is used separately. The sponge and honeycomb combination was found to have a better absorption coefficient than the egg tray and sponge combination.

Fig. 5 shows the frequency dependence of the complex specific acoustic impedance ratio. The real part of the specific acoustic impedance shows a parabolic behavior with most of the absorbing materials having a peak value at a frequency of around 60 Hz, whereas the imaginary component of the impedance ratio has a maximum negative value at a frequency of 70 Hz. After the peak value, the absolute value of the impedance ratio decreases with the frequency for both real and imaginary components. Aluminium has an obvious highest real part of the

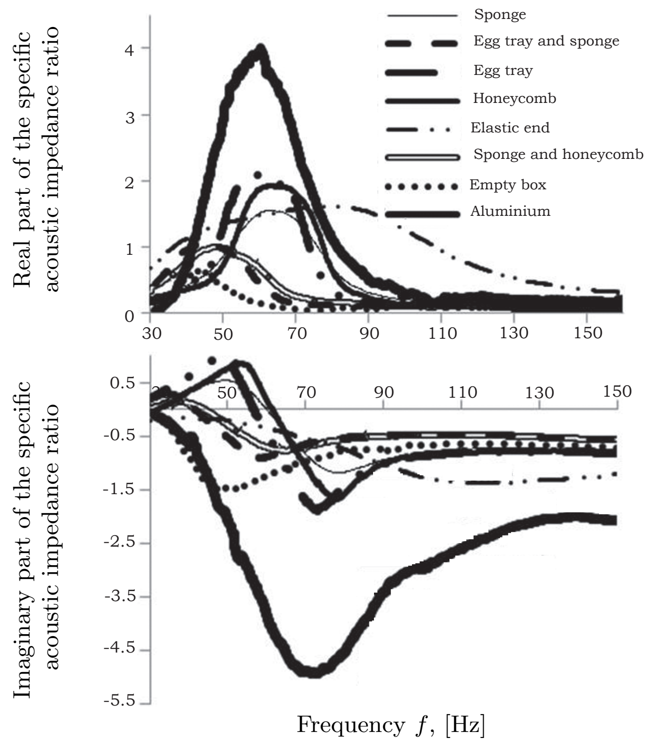

Fig. 5. The comparison of the real and the imaginary part of the specific acoustic impedance ratio for all eight absorbing materials.

impedance ratio, but when the frequency is beyond 80 Hz, the maximum real part of the impedance ratio is found for the elastic end. Conversely, for the imaginary component of the impedance ratio, aluminium has the higher negative imaginary impedance ratio throughout the frequency range. This implies that the aluminium also dissipates some energy at a frequency between 40 to 80 Hz since it is not a perfect rigid end. It can be seen that the elastic end performs fairly well and dissipates more energy compare to all the materials except at the peak region at 40 to 80 Hz. The same behaviour was also found as a result of the absorption coefficient when the elastic end showed the highest absorption coefficient.

In fact, the experimental and DeltaEC results would never be 100 percent identical and correspond to each other. DeltaEC uses the ideal assumptions which do not apply to the real life experiment. The uncertainties of the experiment apparatus are also an important factor in this study. One of the possible errors will be the imperfect sealing between the tubes and the tapers. The tubes and tapers are connected by using several bolts and nuts surrounding the flange with the aid of rubber gaskets. The uneven distribution of tightening forces will definitely cause a certain amount of air leakage, which leads to inaccurate results to be taken. Besides, in order to carry out the microphone calibration, the microphones are slotted in and out every experimental run. It is believed that the rubber and O-rings used to mount the microphones in place are gradually worn out, thus, the further air leakage occurs. Furthermore, the experiment should be carried out in an anechoic room, where the walls, the floor and the ceiling are treated with a wedge-shaped acoustical absorbing material that absorbs the unwanted sound from the surrounding. There is also a certain possibility that unwanted noise was induced when the loudspeaker vibrated and propagated down the tube via the tube surface. Instead of placing the loudspeaker directly on the table, a vibration absorber was placed below the loudspeaker to get rid of the vibration. Moreover, the method used to hold the sample might not be appropriate especially when the elastic end and alumium are under investigation. It is important to ensure that the same amount of force is applied to every single nut to avoid the contribution of the unwanted vibration.

6. Conclusions. The aim of this work was to identify a suitable attenuation for an experimental setup for a low frequency travelling wave thermoacoustic engine. The experimental setup was successfully modelled and simulated with DeltaEC, and the comparison of the two results showed a very good agreement for a rigid end situation. Eight materials and combinations were investigated to realise that using an elastic end will work better for low frequency attenuation applications. The selection of the attenuation material or combination of material should be done carefully and is strongly dependent on the target frequency. None material can work better for all frequencies. Most of the high frequency results are completely inapplicable to low frequency situations. The outcomes of this work will be used for further ongoing investigations on loss assessments of the low frequency thermoacoustic engine. The validated DeltaEC model will be used to investigate a wider range of alternatives for better optimisation. The absorption coefficient can be improved by using a more elastic end; the optimum elasticity requirement will be optimised using a DeltaEC simulation. A compliance volume integrated with an elastic end is also expected to work as a better alternative.

References

[1] G.W. Swift. *A unifying perspective for some engines and refrigerators* (USA, Acoustic Society of America, 2002).

[2] B.M. Chen, Y.A. Abakr, J.H. Goh, P.H. Riley, D.B. Hann. Development and assessment of a SCORE Demo2.1 thermoacoustic engine. *Proc. International Conference on Low-Cost, Electricity Generating Heat Engines for Rural Areas* (Nottingham, UK, 2012).

[3] F.J. Fahy. A simple method for measuring loudspeaker cabinet impedance. *J. Audio Engineering Society*, vol. 41 (1993), pp. 154–156.

[4] A.F. Seybert, D.F. Ross. Experimental determination of acoustic properties using a two-microphone technique. *J. the Acoustical Society of America*, vol. 61 (1977), pp. 1362–1370.

[5] J.Y. Chung, D.A. Blaser. Transfer function method of measuring in-duct acoustic properties. I. Theory. *J. the Acoustical Society of America*, vol. 68 (1980), pp. 907–913.

[6] J.Y. Chung, D.A. Blaser. Transfer function method of measuring in-duct acoustic properties. II. Experiment. *J. the Acoustical Society of America*, vol. 68 (1980), pp. 914–921.

[7] J.Y. Chung, D.A. Blaser. Transfer function method of measuring acoustic intensity in a duct system with flow. II. Experiment. *J. the Acoustical Society of America*, vol. 68 (1980), pp. 1570–1577.

[8] W.T. Chu. Extension of the two-microphone transfer-function method for impedance tube measurements. *J. the Acoustical Society of America*, vol. 80 (1986), pp. 347–348.

[9] T.W. Chu. Transfer-function technique for impedance and absorption measurements in an impedance tube using a single microphone. *J. the Acoustical Society of America*, vol. 80 (1986), pp. 555–560.

[10] B. Hans, A. Mats. Influence of errors on the two-microphone method for measuring acoustic properties in ducts. *J. the Acoustical Society of America*, vol. 79 (1986), pp. 541–549.

[11] A. Mats, B. Hans. Error analysis of two-microphone measurements in ducts with flow. *J. the Acoustical Society of America*, vol. 83 (1988), pp. 2429–2438.

[12] P. Banks-Lee, H. Peng. Length error analysis for impedance tube measurements. *J. the Acoustical Society of America*, vol. 85 (1989, pp.) 1769–1772.

[13] F.G.B. Katz. Method to resolve microphone and sample location errors in the two-microphone duct measurement method. *J. the Acoustical Society of America*, vol. 108 (2000), pp. 2231–2237.

[14] W.T. Chu. Further experimental studies on the transfer-function technique for impedance tube measurements. *J. the Acoustical Society of America*, vol. 83 (1988), pp. 2255–2260.

[15] G.J. Michael, E.S. Patricia. Comparison of methods for determining specific acoustic impedance. *J. the Acoustical Society of America*, vol. 101 (1997), pp. 2694–2704.

[16] W.T. Chu. Impedance tube measurements a comparative study of current practices. *J. the Noise Control Engineering*, vol. 37 (1991), pp. 37–44.

[17] M.G. Jones, T.L. Parrott. Evaluation of a multi-point method for determining acoustic impedance. *Mechanical Systems and Signal Processing*, vol. 3 (1989), pp. 15–35.

[18] S.H. Jang, J.G. Ih. On the multiple microphone method for measuring in-duct acoustic properties in the presence of mean flow. *J. the Acoustical Society of America*, vol. 103 (1998), pp. 1520–1526.

[19] Y. Cho, P.A. Nelson. *Least squares estimation of acoustic reflection coefficient* (Institute of Acoustic Spring Conference, Salford, UK, 2002).

[20] R. Oldfield, F. Bechwati. Accurate low frequency impedance tube measurements. *Proc. the Institute of Acoustics*, vol. 30 (2008), pp. 66–76.

[21] B. Ward, J. Clark, G.W. Swift. *Design environmental for low amplitude thermoacoustic energy conversion* (USA, Los Alamos National Laboratory, version 6.2; 2008).

Received 29.10.2014